Laser and Particle Beams (2012), *30*, 651–657.

doi:10.1017/S0263034612000687

Multiply charged ion emission from laser produced tungsten plasma

B. ILYAS,[1] A.H. DOGAR,[2] S. ULLAH,[2] N. MAHMOOD,[3] AND A. QAYYUM[2]

[1]Department of Metallurgy and Materials Engineering, Pakistan Institute of Engineering and Applied Sciences, Islamabad, Pakistan
[2]Physics Division, Pakistan Institute of Nuclear Science and Technology, Islamabad, Pakistan
[3]Optics Laboratories, Islamabad, Pakistan

(RECEIVED 5 April 2012; ACCEPTED 13 July 2012)

Abstract

Plasma was generated by focusing 10 ns Nd:YAG ($\lambda = 1064$ nm) laser pulse on the thick tungsten target. The laser fluence at the target was varied in the range of 3.57–10.97 J/cm^2. The ion emission from the expanding tungsten plasma was analyzed with the help of an ion collector and time-of-flight electrostatic ion energy analyzer. About 44 times rise in the ion charge per laser shot was observed in the investigated laser fluence range. The measured threshold fluence for onset of the tungsten plasma was 3.27 J/cm^2. The estimated plume expansion coefficient $Z_{inf}/X_{inf} = 2.5 \pm 0.2$ was in agreement with the previous experimental studies and the predictions of self-similar plume expansion model. The electrostatic ion energy analyzer study showed that charge state of the W ions increases with the laser fluence and maximum ion charge state was 5+. It was observed that threshold fluence for appearance of a specific charge state can be measured. A clear correlation between the relative abundances of $W^{(n-1)+}$, W^{n+}, and $W^{(n+1)+}$ indicates that higher order charge states are most probably produced by stepwise ionization process.

Keywords: Highly charged ions; Laser-produced plasma; Plume expansion coefficient; Time-of-flight; Tungsten

1. INTRODUCTION

The production of high density and high temperature plasma by focusing short pulse of laser radiation onto the surface of a solid has attracted increasing amount of interest because of its wide range of applications in various research fields, such as material growth and processing, synthesis of nano-particles, elemental analysis of multi-component materials (Braren *et al.*, 1993) and most importantly the potential source of heavy ions for accelerators and ion implanters (Sharkov *et al.*, 2005). It has been demonstrated (Sellmair & Korschinek, 1988; Láska *et al.*, 1996) that laser-solid interaction process can produce higher current densities of highly charged ions as compared to electron cyclotron resonance ion source, which are presently favored for ion accelerators. Beside the earlier attempts of 1990s (Kutner *et al.*, 1992; Mintsev *et al.*, 1998; Dubenkov *et al.*, 1996), interest in the laser ion source has been recently revived due to the availability of high power Q-switch lasers at a competitive price. For instance, 694 nm ruby laser has been used to produce highly charged Cu^{n+} (n =1–6) ions (Yeates *et al.*, 2010), 1064 nm Nd:glass laser has been utilized to produce ion beam of highly charged Al^{n+} (n = 1–8) ion (Romanov *et al.*, 2010), 1064 nm Nd:YAG laser has been used to generate fully stripped carbon ions (C^{6+}) (Kashiwagi *et al.*, 2004) and recently development of CO_2 laser based plasma generator for injector of C^{4+} ions have been reported (Alekseev *et al.*, 2012).

Various studies have shown that the temperature of the plasma and consequently the ion abundance, ion energy, and charge state distribution depend strongly on the parameters of the incident laser photon such as its wavelength and laser fluence. It appears that only a few times of flight-ion energy analyzer studies regarding effects of the laser fluence on the properties of emitted ions are available in literature (Láska *et al.*, 1996; Burdt *et al.*, 2009; Ilyas *et al.*, 2011) and most of these studies were conducted at very high laser fluence. In addition, none of these studies was conducted on tungsten.

The role of tungsten and its alloys has been emphasized as a possible construction material in high temperature plasma research facilities and fusion reactors. For instance, in JET project tungsten has been anticipated as an alternate material for carbon target plate (Rapp *et al.*, 2010; Mertens *et al.*, 2009). Also tungsten has been proposed as a first wall

Address correspondence and reprint requests to: A. Qayyum, Department of Metallurgy and Materials Engineering, Pakistan Institute of Engineering and Applied Sciences, Islamabad, Pakistan. E-mail: aqayyum11@yahoo

material for international thermonuclear experimental reactor operation (Hirai *et al.*, 2007). Therefore, investigation on the performance of tungsten under intense electromagnetic flux and emission of charged particles from it are of fundamental interest for plasma physicists and engineers. Previously, the effects of applied electric and magnetic field on the laser generated tungsten plasma (Wolowski *et al.*, 2002) and erosion of plasma facing tungsten plates (Beigman *et al.*, 2007) have been investigated by ion collectors and spectroscopic methods, respectively. Several new W^1 and W^2 spectral lines have been identified during these studies. In general, most of the available literature is about the identification of plasma species and the effects of laser parameters on properties of the plasma such as electron temperature, electron density, plasma potential, etc. However, relatively little quantitative information is available on the effect of laser energy on the charge state distribution of tungsten ions, threshold fluence for ion detection and angular distribution of tungsten ions. The lack of experimental data on these important parameters have precluded satisfactory modeling of the expanding laser plasma as well as its application as a source of ions for particle accelerators. Therefore, the main aim of this study was to investigate ion emission from tungsten target as a function of the laser fluence. In particular, we present energy resolved times of flight spectra of the tungsten ions, and a detailed analysis of the relative abundance of various ion charge states as a function of the incident laser fluence. We also measured total ion charge, angular distribution of ion charge, and estimated threshold fluence for ion production and expansion ratio of the tungsten plasma.

2. EXPERIMENTAL SETUP

The experimental setup used for generation and diagnostics of W ions is described in detail elsewhere (Ilyas *et al.*, 2011). The experimental setup consist mainly of an Nd:YAG laser with associated beam delivery optics, ablation chamber, electrostatic lens, time-of-flight (TOF) ion energy analyzer, ion detection, and electronic system for data acquisition (Fig. 1). The pulsed radiation from an Nd:YAG laser (wavelength = 1064 nm, pulse duration about 10 ns) is focused by an optical lens (focal length $f = 50$ cm) onto the surface of a high purity (99.99%) tungsten target. Laser beam enters the vacuum system through a quartz window and impinge on the target at an angle of 45° with respect to the target surface normal. A direct current motor

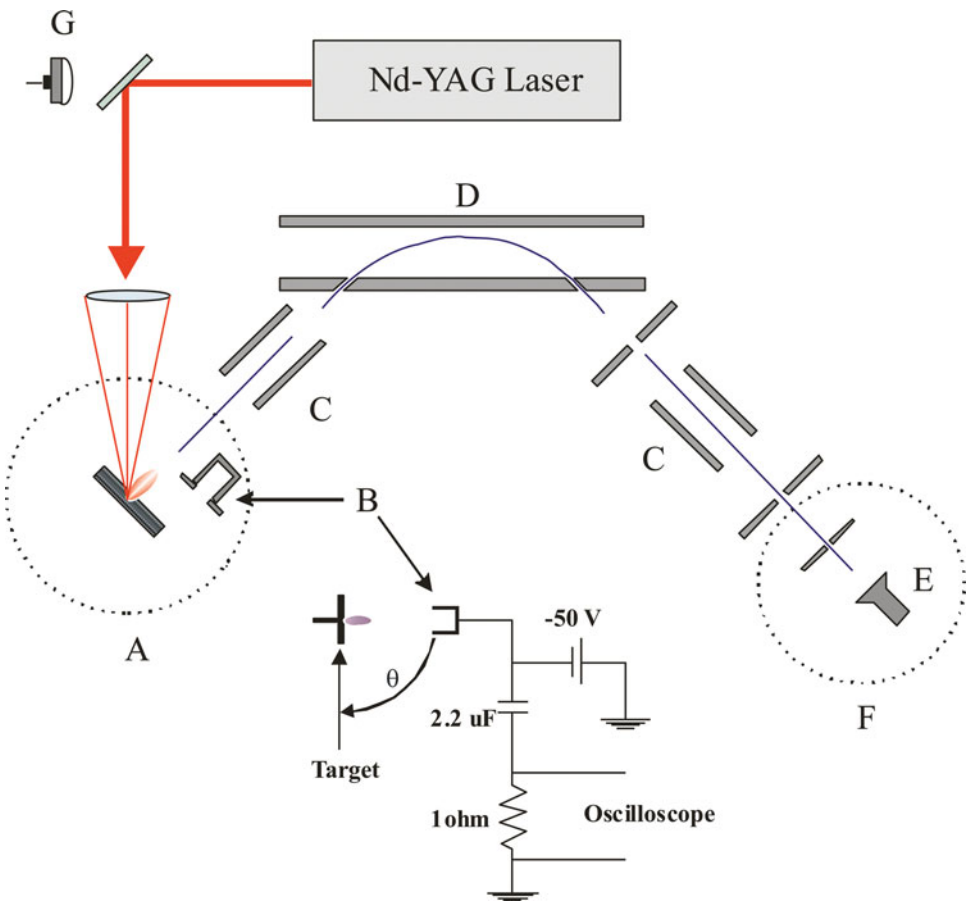

Fig. 1. (Color online) Schematic of the experimental setup. (**A**) ablation chamber, (**B**) ion collector, (**C**) Einzel lens, (**D**) 45° parallel plate electrostatic ion energy analyzer, (**E**) channel electron multiplier, (**F**) ion detection chamber, and (**G**) Photodiode. Experimental arrangement for the ion collector measurement along with the electrical circuit is also shown.

https://doi.org/10.1017/S0263034612000687 Published online by Cambridge University Press

continually rotates the target at about 100 rpm so that each laser shot strikes the fresh surface. Also target can be moved vertically with the help of a vacuum feed through that permits to change the spot position. The area (7.85×10^{-3} cm^2) of slightly elliptical laser spot on the target surface was inferred by analysis of the crater using optical microscope. The laser fluence at the target was varied in the range of 3–11 J/cm^2 by changing the laser energy.

The plasma expansion is monitored by a cylindrical ion collector (Faraday Cup) placed along the target surface normal at a distance of 6.5 cm from the target (see Fig. 1). The ion collector (IC) has a circular aperture of 10 mm in diameter. While a grounded aperture of the same diameter was placed before the IC. The IC is biased with −50 V to repel electrons emitted from the laser plasma. The IC signal was determined from the voltage drop across a 1 Ω resistor with the help of a fast digital storage oscilloscope (1 GHz bandwidth). The IC measures a time-resolved ion signals during the plasma expansion (see Fig. 2), from which the total ion charge and the average ion energy can be obtained. Before entering the electrostatic energy analyzer (EEA) a drift distance of 45 cm is provided for plume expansion. This distance is within the range of typical drift distances recommended for the laser ion sources (Sharkov, 1995). The EEA consists of two parallel plates, the front plate is grounded and back plate is at some applied potential V_a. Ions are admitted through the entrance slit of width $w = 2$ mm at some initial energy and charge state E_i/q_ie and subsequently decelerated by the constant electric field of $-V_a/d$ between the plates, where d is the distance between the plates is 35 mm. In this configuration, only ions with a particular energy and charge state leave the device through the 2 mm wide exit slit. The distance L between the entrance and exit slit of this device is 103 mm. The energy resolution

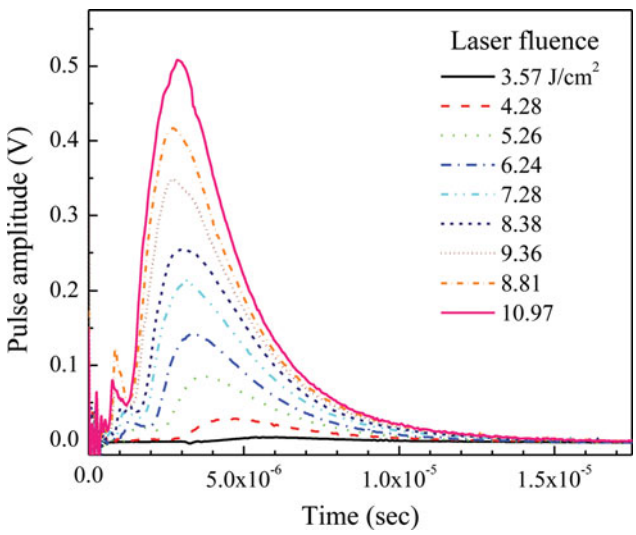

Fig. 2. (Color online) TOF ion signals measured by the ion collector for various values of the laser fluence. Ion collector was placed at a distance of 6.5 cm along the target surface normal.

of this device is given as (Hofer *et al.*, 1999):

$$\frac{\Delta E_i}{E_i} \approx \frac{\sqrt{2}W}{2L} = 1.4\%. \quad (1)$$

The ions were detected by means of a channel electron multiplier (CEM), whose signal is acquired by a fast digital storage oscilloscope (1 GHz bandwidth). A fast photodiode is used to trigger the oscilloscope at the time laser hits the target. The flight distance of ions from target to the CEM is 1.31 meter. This whole arrangement provides energy resolved TOF mass spectra of the positively charged ions ablated by a laser shot, which can be used to determine mass-to-charge ratios, ion energies and abundance. The energy of the ions reported in this experiment is in the range of about 0.6–3 keV (see Fig. 5). In this ion energy range, the increase in detection efficiency of CEM is about 2.3%, which has been incorporated while evaluating the relative abundance of the ions. The Einzel lenses placed before and after the EEA are used to manipulate or optimize the signal of a specific ion charge state. But these Einzel lenses are placed at ground potential during this study. The experiments are conducted in vacuum below 10^{-6} torr to minimize the charge exchange with the ambient residual gas.

3. RESULTS AND DISCUSSION

The TOF ion signals detected by negatively biased (−50 V) ion collector placed at a distance of 6.5 cm along the target surface normal are shown in Figure 2. For this measurement, laser fluence was varied in the range of 3.57 to 10.97 J/cm^2. Each curve is the average of IC signal measured for three consecutive laser shots. These broad ion pulses were generated by narrow laser shots of 10 ns duration. Following trends can be seen in the experimental results presented in Figure 2; (1) For each value of laser fluence, the ion current attains a maximum value and then decreases as the plume continues to expand beyond the ion collector, (2) the height of ion pulse increases with the laser fluence, (3) the position of peak shifts to shorter times as the laser fluence increases indicating the increase in average energy of the ion pulse, and (4) the low intensity peaks before the main peak for each value of laser irradiance are most probably due to target surface contaminations like oxygen, carbon, hydrogen and hydrocarbons. The total ion charge per pulse for various values of laser fluence was evaluated by integrating the corresponding TOF ion spectra shown in Figure 2:

$$\int_{t_i}^{t_f} V(t)dt = \int_{t_i}^{t_f} RI(t)dt = \int_{t_i}^{t_f} R\frac{dQ}{dt}dt = R\int_{Q_i}^{Q_f} dQ = RQ, \quad (2)$$

$$Q = \frac{\int_{t_i}^{t_f} V(t)dt}{R}, \quad (3)$$

where R is the load resistance, Q_i and Q_f, respectively are the charge values corresponding to the start and the end of TOF

https://doi.org/10.1017/S0263034612000687 Published online by Cambridge University Press

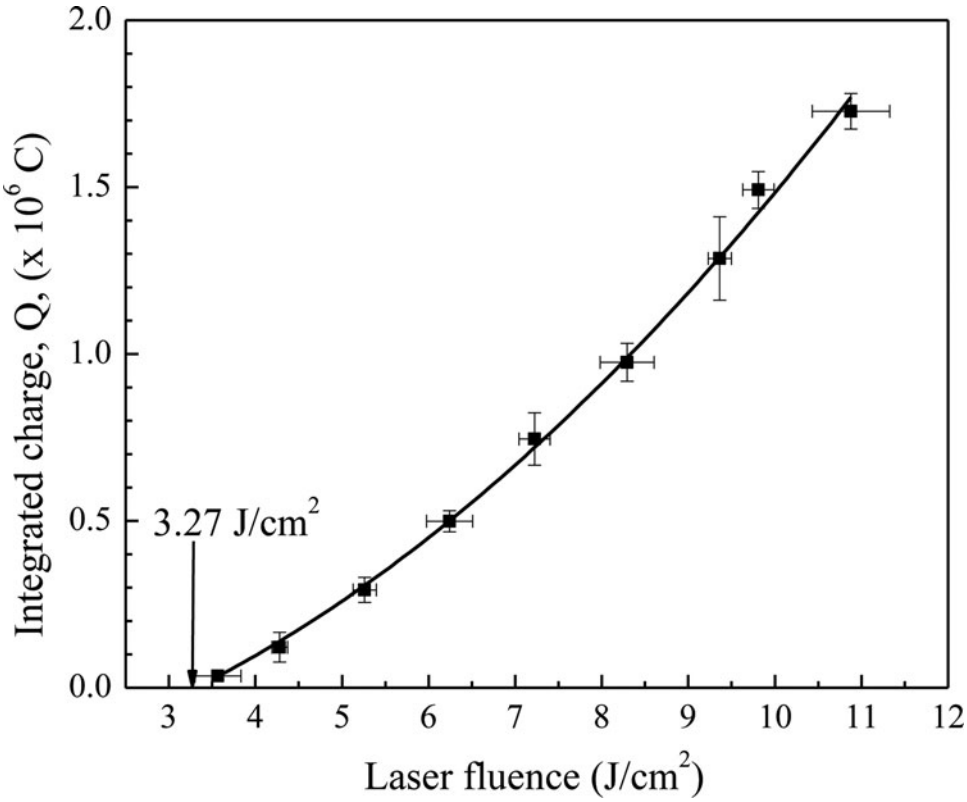

Fig. 3. Integrated ion charge as a function of the laser fluence. Vertical arrow shows the estimated threshold fluence for the onset of the ion signal. Smooth curve is the polynomial fit to the data points.

signal and I is the instantaneous ion current. The total ion charge so obtained is plotted as a function of the laser fluence in Figure 3. The vertical error bars indicate statistical error of total ion charge measured for three laser shots. Whereas horizontal error bars give shot to shot variation of the measured laser fluence. The smooth curve in Figure 3 shows polynomial fit to the experimental data points. Consistent with previous studies of silver (Margarone *et al.*, 2008) and Al_2O_3 ablation with Nd-YAG laser of wavelength 1064 nm and 532 nm (Caridi *et al.*, 2009), respectively, total ion charge increases with the laser fluence. Figure 3 shows about 44 times rise in total ion charge while the laser irradiance was increased just three times. This behavior may be due to two simultaneous effects. First is the amount of material ablated from the target increases with the laser fluence. Second is the laser energy deposited in the vapor increases that cause efficient heating of the plasma. The threshold fluence $F_{th} = 3.27\ \mathrm{J/cm^2}$, the minimum fluence needed to detect charged species in 1064 nm Nd-YAG laser produced tungsten plasma was obtained by extrapolating the curve in Figure 3 to $Q = 0$. To the best of our knowledge threshold fluence for tungsten is not available for comparison. However, threshold fluence of few metals at various laser photon wavelengths has been reported (see Table 1). It can be seen that threshold fluence of tungsten is slightly high as compared to the copper and aluminum. According to the simple laser ablation model (Amoruso *et al.*, 1998), F_{th} for the target irradiated with laser pulse of duration t_p is given as

Table 1. *The threshold laser fluence of various target materials*

Target material	Wavelength of laser photon (nm)	Threshold fluence ($\mathrm{J/cm^2}$)
W (this study)	1064	3.27
Cu (Ilyas *et al.*, 2011)	1064	2.5
Cu (Amoruso *et al.*, 1998)	351	2
Al (Torrisi *et al.*, 2006)	532	2.08

$$F_{th} \propto \frac{1}{(1-R)}\sqrt{\frac{\chi t_p^2 \rho C_p T_v^2}{t_v}}. \quad (4)$$

Where R is the reflectivity, χ is the thermal conductivity, ρ is the target density, C_p is the specific heat, t_v is the time taken to reach the threshold temperature beyond, which vaporization takes place and T_v the vaporization temperature of the target material. Reflectivity of tungsten for 1064 nm laser photon (Benavides *et al.*, 2011) and its thermal conductivity is less than that of copper. But the vaporization temperature and density of tungsten is significantly high as compared to both copper and aluminum. Therefore, relatively high

https://doi.org/10.1017/S0263034612000687 Published online by Cambridge University Press

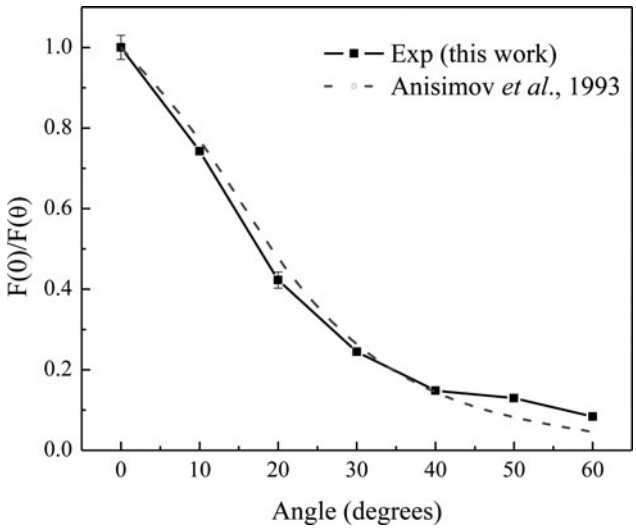

Fig. 4. The angular distribution of normalized ion yield. The dotted line is best fit of Eq. (5) to the experimental data.

threshold fluence of tungsten is most probably due to the combined effect of high vaporization temperature and density.

In order to measure the angular distribution of ion charge in front of the target surface, TOF ion spectra were recorded by placing IC at various angles with respect to the target surface normal. While target to IC distance was kept fixed at 6.5 cm. The total ion charge at various angles, $F(\theta)$, was determined by integration of TOF spectra recorded at various angles. The normalized ion distribution $F(\theta)/F(0)$ is plotted in Figure 4. Where *F(0)* is the ion charge at $\theta = 0°$. It can be seen that ion charge decreases with the angle and at $\theta = 60°$ it is decreased by an order of magnitude. Anisimov *et al.* (1993) proposed a three-dimensional isentropic and adiabatic self-similar expansion of the laser plume at the end of the laser pulse. Initially, plume is a small semi-ellipsoidal volume of hot material with dimensions X_0, Y_0, and Z_0, where Z_0 is the normal to the target. According to this model (Anisimov *et al.*, 1993) the normalized angular distribution of the ablated atoms in the *X-Z* plane for the expansion time of the order of microsecond is give as

$$\frac{F(\theta)}{F(0)} = \left(1 + \tan^2\theta\right)^{3/2}\left[1 + \left(\frac{Z_{\inf}}{X_{\inf}}\right)^2 \tan^2\theta\right]^{-3/2}. \qquad (5)$$

Where Z_{inf} and X_{inf} are the values of Z and X, respectively, at $t \to \infty$. The asymptotic ratio $Z_{\inf}/X_{\inf}$ is therefore a measure of the forward peaking of the laser plume. Sometimes it is also referred to as the plume expansion ratio. The best fit of Eq. (5) to the experimental data presented in Figure 4, which provides a value of asymptotic ratio $Z_{\inf}/X_{\inf} = 2.5 \pm 0.2$. The close agreement of experimental results in

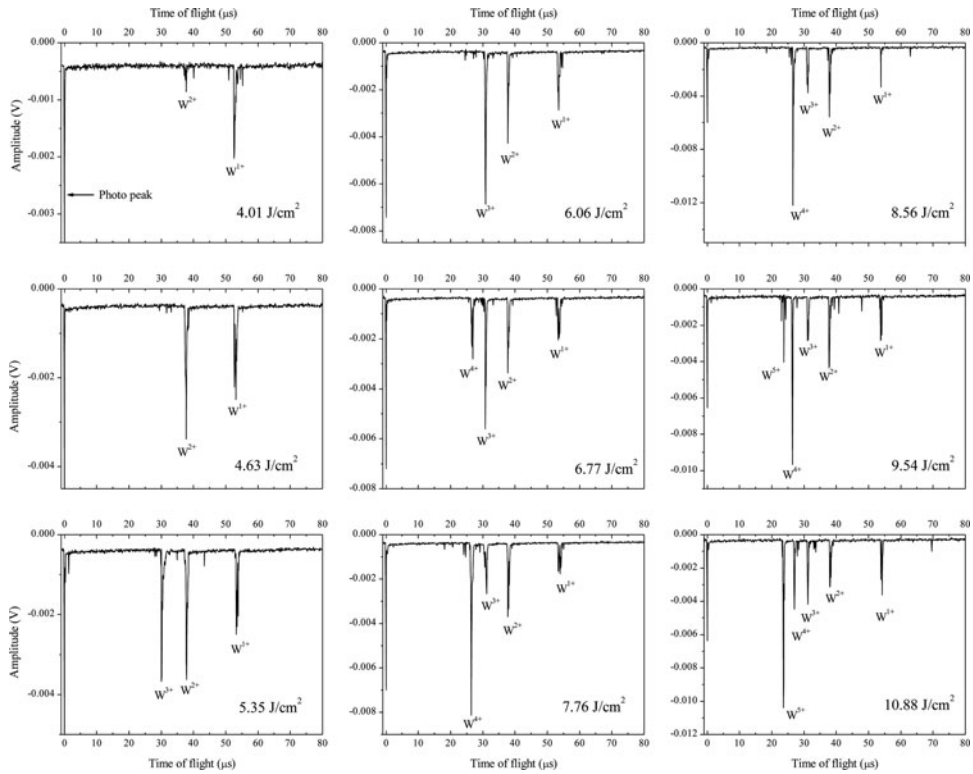

Fig. 5. TOF ion energy analyzer spectra obtained by irradiating a W target with various values of the laser fluence. For these measurements filtering criterion of the ion energy analyzer was fixed at $E/q = 574$ eV/charge. Note that vertical axes scale of the various graphs is not same.

https://doi.org/10.1017/S0263034612000687 Published online by Cambridge University Press

Eq. (4) indicates that the expansion of laser produced tungsten plasma can be described by the Anisimov model. Previously, expansion ratio has been experimentally estimated for a number of target materials with the laser beams of various wavelengths and fluences. The data shown in Table 2 indicates that plume expansion ratio does not seem to depend on the laser or material properties.

Previously the expansion ratio has been experimentally estimated for various target materials, for instance, with a 355 nm Nd-YAG laser a value of 2.2 for Ag at a fluence of 0.8 J/cm^2 (Hansen *et al.*, 1999), 2.2 for Cu and Ni at fluence of 2.5 J/cm^2 and 3.0 for Zn at the fluence of 0.8 J/cm^2 (Thestrup *et al.*, 2002) have been reported. Such an ion distribution (Fig. 4) has important implications for the extraction of ions from laser produced plasma and on the properties of the thin film deposited by pulsed laser deposition. Therefore, in laser ion source, one has to place extractor along the target surface normal to maximize the ion current. As regard the pulsed laser deposition, high flux of energetic ions (energies up to few keV) along the target surface normal can re-sputter already deposited film and can also be implanted deep into the substrate. Therefore, one can expect that properties of the films deposited on the substrates placed at various angle will be different.

Next, we analyzed the charge state distribution of the tungsten ions as a function of the laser fluence. The TOF ion energy analyzer spectra recorded as a function of the laser fluence are shown in Figure 5. The filtering criterion of the ion energy analyzer was fixed at $E/q = 574$ eV/charge. Ion signals were detected with the help of CEM. The ion peaks in Figure 5 are negative because output of CEM is electron current that was converted to voltage by passing it through a resistor. The first narrow peak in each spectrum at time $t = 0$ is a photo-peak, which is due to the reflection of plasma ultraviolet radiation from the back plate of electrostatic energy analyzer to the channel electron multiplier. At the laser fluence of 4.01 J/cm^2, which is slightly higher than the ablation threshold, the plume consists predominantly of W^{1+} ions however there is an evidence of W^{2+} ions. At the laser fluence of 4.63 J/cm^2, W^{2+} became more abundant as compared to W^{1+}. As the laser fluence was further

Table 2. *The expansion ratio of the metal plumes produced by laser photons of various wavelengths*

Target material	Wavelength of laser photon (nm)	Laser fluence (J/cm^2)	Expansion ratio
W (this study)	1064	10.88	2.5
Cu (Dogar *et al.*, 2011)	1064	13	2.1
Cu (Thestrup *et al.*, 2002)	355	2.5	2.2
Ni (Thestrup *et al.*, 2002)	355	0.8	3.0
Bi (Thestrup *et al.*, 2002)	355	1.0	3.2
Ag (Hansen *et al.*, 1999)	355	0.8	2.2
Ag (Mannion *et al.*, 2005)	775	5.0	2.2

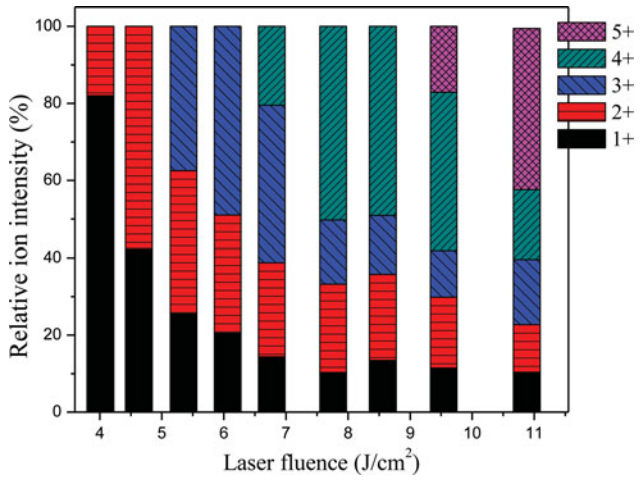

Fig. 6. (Color online) Relative abundance of the various charge states of W ions as a function of the laser fluence.

increased tungsten ions with higher charge state start to appear in a regular fashion. These results clearly indicate that the appearance threshold of various charge states can be found by fine tuning of the laser fluence. The relative intensity of various charge states obtained by integration of these ion peaks is shown in Figure 6. It can be seen that intensity of every charge state rises to a maximum value and then decreases rather slowly with the increase of laser fluence. In addition, percentage increase of W^{2+} is well correlated with the decrease of W^{1+}. Similar correlation in the intensity variation of W^{2+} and W^{3+} also exist. These correlations indicate that the formation of W^{n+} most probably occur through ionization of $W^{(n-1)+}$ by impact of the fast electrons or by multiphoton interactions rather than the direct processes. In general, higher laser fluence produced higher charge states and maximum attainable ion charge state increases with the laser fluence. These results also indicate that the ion charge state distribution of the laser plasma can be controlled by tuning of the laser fluence.

4. CONCLUSION

Ion collector and TOF electrostatic ion energy analyzer was used to diagnose the 1064 nm Nd:YAG laser produced tungsten plasma. Various plasma parameters such as variation of total ion charge as a function of the laser fluence, threshold fluence for onset of the tungsten plasma and angular distribution of the ion charge in front of the target was measured with the help of an ion collector. Slightly higher threshold fluence of tungsten as compared to the copper and aluminum is most probably due to the combined effect of high vaporization temperature and density of the tungsten. But the plume expansion ratio does not seem to depend on the laser or material properties. The study performed with the electrostatic ion energy analyzer showed that maximum attainable charge state increases with the laser fluence and threshold fluence for appearance of a specific charge state can be

https://doi.org/10.1017/S0263034612000687 Published online by Cambridge University Press

measured. Most importantly we identified a correlation between relative abundances of various charge states, which points towards the stepwise ionization of these ions. These results are quite important for the fraternity of scientists working on the development of laser ion sources as well as fundamental understanding of the laser plasma.

REFERENCES

Alekseev, N.N., Balabaev, A.N., Vasilyev, A.A., Satov, Y.A., Savin, S.M., Sharkov, B.Yu., Shumshurov, A.V. & Roerich, V.C. (2012). Development of laser-plasma generator for injector of C^{4+} ions. *Laser Part. Beams* **30**, 65–73.

Amoruso, S., Berardi, V., Bruzzese, R., Spinelli, N. & Wang, X. (1998). Kinetic energy distribution of ions in the laser ablation of copper targets. *Appl. Surf. Sci*. **127–129**, 953–958.

Anisimov, S.I., Bäuerle, D. & Luk'yanchuk, B.S. (1993). Gas dynamics and film profiles in pulsed-laser deposition of materials. *Phys. Rev. B* **48**, 12076–12081.

Beigman, I., Pospieszczyk, A., Sergienko, G., Tolstikhina, I.Yu. & Vainshtein, L. (2007). Tungsten spectroscopy for the measurement of W-fluxes from plasma facing components. *Plasma Phys. Contr. Fusion* **49**, 1833–1847.

Benavides, O., Lebedeva, O. & Golikov, V. (2011). Reflection of nanosecond Nd:YAG laser pulses in ablation of metals. *Opt. Expr*. **19**, 21842–21848.

Braren, B., Bukoski, J. & Norton, D. (1993). *Laser Ablation in Material Processing and Applications*. Pittsburgh: Material research Society.

Burdt, R.A., Yuspeh, S., Sequoia, K.L., Tao, Y., Tillack, M.S. & Najmabadi, F. (2009). Experimental scaling law for mass ablation rate from a Sn plasma generated by a 1064nm laser. *J. Appl. Phys*. **106**, 0333101–0333105.

Caridi, F., Torrisi, L., Mezzasalma, A.M., Mondio, G. & Borrielli, A. (2009). Al_2O_3 plasma production during pulsed laser deposition. *Eur. Phys. J. D*. **54**, 467–472.

Dogar, A.H., Ilyas, B., Qayyum, H., Ullah, S. & Qayyum, A. (2011). Angular distributions of flux and energy of the ions emitted during pulsed laser ablation of copper. *Eur. Phys. J. Appl. Phys*. **54**, 10301–10304.

Dubenkov, V., Sharkov, B., Golubev, A., Shumshurov, A., Shamaev, O., Roudskoy, I., Sireltov, A., Satov, Y., Makarov, K., Smakovsky, Y., Hoffmann, D., Laux, W., Muller, R.W., Spaedtke, P., Stöckl, C., Wolf, B. & Jakoby, J. (1996). Acceleration of Ta^{+10} ions produced by laser ion source in RFQ MAXILAC. *Laser Part. Beams* **14**, 385–392.

Hansen, T.N., Schou, J. & Lunney, J.G. (1999). Langmuir probe study of plasma expansion in pulsed laser ablation. *Appl. Phys. A* **69**, S601–S604.

Hirai, T., Maier, H., Rubel, M., Mertens, Ph., Neu, R., Gauthier, E., Likonen, J., Lungu, C., Maddaluno, G., Matthews, G.F., Mitteau, R., Neubauer, O., Piazza, G., Philipps, V., Riccardi, B., Ruset, C., Uytdenhouwen, I. & JET EFDA Contributors. (2007). R&D on full tungsten divertor and beryllium wall for JET ITER-like wall project. *Fusion Engineering and Design* **82**, 1839–1845.

Hofer, R., Hass, J. & Gallimore, A. (1999). *Proc. 26th Int. Conf. on Electric Propulsion*. Kitakyushu. Japan.

Ilyas, B., Dogar, A.H., Ullah, S. & Qayyum, A. (2011). Laser fluence effects on ion emission from a laser-generated Cu plasma. *J. Phys. D: Appl. Phys*. **44**, 295202-1/295202-6.

Kashiwagi, H., Hattori, T., Hayashizaki, N., Yamamato, K., Takahashi, Y. & Hata, T. (2004). Nd-Yag laser ion source for direct injection scheme. *Rev. Sci. Instum*. **75**, 1569–1571.

Kutner, V.B., Bykovsky, Y.A., Gusev, V.P., Kozyrev, Y.P. & Peklenkov, V.D. (1992). The laser ion source of multiply charged ions for the U-200 LNR JINR cyclotron. *Rev. Sci. Instrum*. **63**, 2835–2837.

Láska, L., Krása, J., Mašek, K., Pfeifer, M., Trenda, P., Králiková, B., Skála, J., Rolena, K., Woryna, E., Farny, J., Parys, P., Wołowski, J., Mróz, W., Shumshurov, A., Sharkov, B., Collier, J., Langbein, K. & Haseroth, H. (1996). Multiply charged ion generation from NIR and visible laser produced plasma. *Rev. Sci. Instum*. **67**, 950–952.

Mannion, P., Favre, S., O'Connor, G.M., Doggett, B. & Lunney, J.G. (2005). Langmuir probe study of plasma expansion in femtosecond pulsed laser ablation of silver. *Proc. SPIE* **5827**, 457–466.

Margarone, D., Torrisi, L., Borrielli, A. & Caridi, F. (2008). Silver plasma by pulsed laser ablation. *Plasma Sour. Sci. Technol*. **17**, 035019-1/035019-7.

Mertens, Ph., Altmann, H., Hirai, T., Philipps, V., Pintsuk, G., Rapp, J., Riccardo, V., Schweer, B., Uytdenhouwen, I. abd Samm, U. (2009). Development and qualification of a bulk tungsten divertor row for JET. *J. Nucl. Mat*. **390–391**, 967–970.

Mintsev, V., Gryaznov, V., Kulish, M., Fortov, V., Sharkov, B., Golubev, A., Fertman, A., Stöckl, C. & Gardes, D. (1998). On measurements of stopping power in explosively driven plasma targets. *Nucl. Instr. Meth. A* **415**, 715–719.

Rapp, J., Pintsuk, G., Mertens, Ph., Altmann, H., Lomas, P.J. & Riccardo, V. (2010). Geometry and expected performance of the solid tungsten outer diverter row in JET. *Fusion Engin. Desig*. **85**, 153–160.

Romanov, V.I., Rupasov, A.A., Shikanov, A.S., Paperny, V.L., Moorti, A., Bhat, R.K., Naik, P.A. & Gupta, P.D. (2010). Energy distributions of highly charged ions escaping from a plasma via a low-voltage laser-induced discharge. *J. Phys. D: Appl. Phys*. **43**, 465202-1/465202-7.

Sellmair, J. & Korschinek, G. (1988). The Munich laser ion source. *Nucl. Instr. Meth. A* **268**, 473–477.

Sharkov, B. (1995). *Handbook of Ion Sources*. Boca Raton: Chemical Rubber, 149.

Sharkov, B.Y. & Scrivens, R. (2005). Laser ion sources. *IEEE Trans. Plasma Phys*. **33**, 1778–1785.

Thestrup, B., Toftmann, B., Schou, J., Doggett, B. & Lunney, J.G. (2002). Ion dynamics in laser ablation plumes from selected metals at 355nm. *Appl. Surf. Sci*. **197–198**, 175–180.

Torrisi, L., Caridi, F., Picciotto, A. & Borrielli, A. (2006). Energy distribution of particle ejected by laser-generated aluminum plasma. *Nucl. Instr. Meth. B* **252**, 183–189.

Wolowski, J., Celona, L., Ciavola, G., Gammino, S., Krása, J., Láska, L., Parys, P., Rohlena, K., Torrisi, L. & Woryna, E. (2002). Expansion of tungsten ions emitted from laser-produced plasma in axial magnetic and electric fields. *laser Part. Beams* **20**, 113–118.

Yeates, P., Costello, J.T. & Kennedy, E.T. (2010). The DCU laser ion source. *Rev. Sci. Instum*. **81**, 043305-1/043305-10.